Transcriptomics effects of per- and polyfluorinated alkyl substances in differentiated neuronal cells

Logan Running[1], Charikleia Karageorgiou[2], Michele Camdzic[1], Omer Gokcumen[2], Diana S. Aga[1,*], G. Ekin Atilla-Gokcumen[1,*]

[1]Department of Chemistry, University at Buffalo, The State University of New York (SUNY), Buffalo, NY USA 14260

[2]Department of Biological Sciences, University at Buffalo, The State University of New York (SUNY), Buffalo, NY USA 14260

Abstract:

Per- and polyfluorinated alkyl substances (PFAS) are ubiquitous in most environments, accumulate in several tissues, and can adversely affect human health. PFAS have been implicated in neurodegenerative and behavioral disorders. However, the mechanisms through which PFAS affects biological function in neurons mostly remain unknown. In this study, SH-SY5Y neuroblastoma cells were used to study the effect of perfluorooctanoic acid (PFOA), perfluorooctansulfonic acid (PFOS), perfluorodecanoic acid (PFDA), perfluorodecanesulfonic acid (PFDS), 8:2 fluorotelomer sulfonate (8:2 FTS) and 8:2 fluorotelomer alcohol (8:2 FTOH) exposures on neuronal health. After a 30 μM-, 24-hour exposure, cells accumulated up to 800 ng PFAS/mg protein. Transcriptomics analysis of control and PFAS-exposed cells revealed 721 genes were differentially expressed across six treatments ($p_{adj} < 0.05$). Eleven of these differentially expressed genes were observed for all treatments, suggesting that these genes are potential markers for neuronal PFAS exposure. In PFOA-treated cells, we observed multiple downregulated genes are enriched for functions related to synaptic growth and neural function. In contrast, upregulated genes in PFOS, PFDS, FTS, and FTOH-treated cells showed enrichment in functions related to response to hypoxia and amino acid metabolism, suggesting PFAS impact different cellular processes in neuronal cells based on their chemical composition and structure. Consistent with this observation, analysis of major lipid classes after exposure to select PFAS showed significant upregulation of fatty acids with PFDA, PFDS and 8:2 FTS and downregulation of triacylglycerols with 8:2 FTOH exposure. Overall, these results suggest that PFAS induce different effects *in vitro* depending on their chemical structures and specific biological processes that potentially underlie negative effects of PFAS on neuronal health.

Keywords: PFAS, biomarker, RNA-seq, neuronal differentiation, neurotoxicity

Synopsis:

Per- and poly fluorinated alkyl substances (PFAS) have been shown to bioaccumulate in human tissues and affect health. This study aims to provide insight into the specific biological processes by which PFAS exposure affects neuronal cells.

INTRODUCTION

Per- and poly fluorinated alkyl substances (PFAS) are a class of chemical contaminants of global concern. PFAS has been commonly studied in recent years; however, the environmental burden and human health impact of these compounds are still not fully understood. A recent study in the United States (US) showed detectable levels of PFAS in serum samples from most participants (97%), highlighting the ubiquitous presence of these compounds in the environment and the risk of human exposure.[1] Monitoring efforts in the past few decades resulted in some positive trends towards phasing out certain legacy PFAS, such as perfluorooctanoic acid (PFOA) and perfluorooctane sulfonic acid (PFOS).[2, 3] However, the US Environmental Protection Agency (EPA) reports that tens of thousands of tons of PFAS-containing materials are still produced globally each year.[4] These include linear or branched alkyl short-chain PFAS, which are fully or partially fluorinated with ether, alcohol, sulfonates, or carboxylate headgroups, among others.[5]

PFAS exposure is particular relevant to epidemiology of humans because of inherent chemical stability[6, 7] and fat solubility[8] of PFAS. A study in mice found that radiolabeled PFOA, perfluorohexanoic acid (PFHxA) and perfluorobutanoic acid (PFBA), were detected four hours after administration in every organ, including the brain.[9] Further, the extended serum half-lives of PFAS (months to a year for short chain[10] – up to 5 years for long chains[11]) lead to their bioaccumulation in humans. While certain professions are at an increased risk for PFAS exposure including firefighters, industrial workers and ski board waxers, general communities are also at risk from PFAS, the ones found in our water sources, food packing and cosmetics.[12]

PFAS affect many systems and processes, including the endocrine system[14, 15], menstrual cycle, sperm mobility, and the age of onset puberty.[16] The liver accumulation of PFAS is common, and hepatoxicity has been observed in human studies.[17, 18] The exact mechanism of liver toxicity is unknown; however, PFOS/PFOA exposures have been shown to trigger peroxisome proliferator-activated receptor alpha (PPAR-α).[19, 20] Certain cancers such as liver, prostrate or testicular cancer have been linked to PFAS mediated PPAR-α disruption and epigenetic changes.[21, 22]

PFAS can also cross the blood-brain-barrier and are detected in brain tissue and cerebrospinal fluid.[23, 24] Perfluorocarboxylates and perfluorosulfonates with 6-14 carbon chains were detected in rodents, fish, and bears, with the longer chain PFAS generally occurring at higher concentrations.[25] Further, PFHxA and PFBA have been detected in brain tissues up to 300 ng/g in humans[13]. A recent study found PFOA, perfluorohexane sulfonic acid (PFHxS), PFHxA in various parts of the male brain, with levels correlated strongly with PFAS levels in respective blood samples from these individuals. Surprisingly, the same study showed that low levels of PFOS in the blood and not in the brain, indicating selective accumulation of different PFAS in the brain.[26]

Previous studies have suggested that PFAS transport into the brain across BBB could be mediated by lipid transporters[27], other organic anionic transporter,[28] and the disruption of the BBB[29]. Multiple potential routes of exposure, evidence of PFAS accumulation in the brain, and the myriad types of PFAS prevalent in the environment could suggest an underreported high risk of PFAS exposure.

Examples of suspected neurotoxic impacts of PFAS in humans extend to behavioral and neurodegenerative disorders. Studies have linked PFAS neurotoxicity to changes in neurotransmitter levels and disruption of synaptic homeostasis, which in turn, can serve as risk factors for neurodegenerative diseases, such as Alzheimer's or Parkinson's disease.[30, 31] Further, infant exposure of PFAS during pregnancy and childhood through the mothers' blood and breast milk have been linked to dysregulations in childhood physiology and behavior.[32, 33] PFOS, PFHxS, and perfluorononanoic acid (PFNA) are linked to several symptoms of attention deficit hyperactivity disorder (ADHD), such as hyperactivity and aggression. In contrast, PFHxS was correlated with internalizing behavior such as depression and anxiety.[34] However, the mechanism that underlie these negative effects of PFAS are unknown.

In this study, we investigated the neurotoxic effects of PFAS in differentiated SH-SY5Y cells, using changes in gene expression as a primary method. The SH-SY5Y cell line is a neuroblastoma cell line and can be differentiated into neuronal cells over an 11-day period.[35] We used differentiated SH-SY5Y cells to evaluate the changes in the transcriptome after exposure to six different long-chain (8-10 carbons) PFAS, (PFOA), perfluorooctansulfonic acid (PFOS), perfluorodecanoic acid (PFDA) perfluorodecanesulfonic acid (PFDS), 8:2 fluorotelomer sulfonic acid (8:2 FTS) and 8:2 fluorotelomer alcohol (8:2 FTOH) at 30 μM. We used a 24-hour treatment at sub-toxic concentrations that are higher than environmentally relevant concentrations of these contaminants to achieve cellular levels similar to *in vivo* accumulation of these compounds. Transcriptomics analysis revealed different impacts of PFAS tested at the gene expression levels, with PFOA inducing the highest number of differentially expressed genes ($p_{adj} < 0.05$). Gene enrichment analyses suggested different biological processes that might be perturbed by treatment with different PFAS, including neuronal function, cellular metabolism, and generation of ROS. Analysis of abundant lipid classes before and after exposure showed different lipids to be impacted by different PFAS, consistent with structure-dependent effects we observed at the transcriptomic level.

MATERIALS AND METHODS

Materials

PFOA, PFOS, PFDA, PFDS, 8:2 FTOH, and 8:2 FTS were purchased from Millipore Sigma® (Burlington, MA). M4PFOS and M4PFOS (C13 isotopically labeled standards) were purchased from Wellington Laboratories (Guelph, ON). Ammonium acetate, LC-MS grade methanol and HPLC grade methanol were purchased from J.T. Baker® (Radnor Township, PA). Dansyl chloride was purchased from Fluka Chemical (Buchs, Switzerland). Dimethyl amino pyridine (DMAP), and *N, N*-diisopropyl ethyl amine were purchased from Sigma Aldrich (St. Louis, MO). HPLC grade acetonitrile was purchased from Supelco (Bellefonte, PA). Ethyl acetate was purchased from Avantor (Radnor, PA). Sep-Pak® Vac 6cc (1g) solid phase extraction (SPE) cartridges were purchased from Waters (Milford, MA).

SH-SY5Y neuroblastoma cells were purchased from the American Type Culture collection (Manassas, VA). Dulbecco's modified Eagle media (DMEM) / Hams-F12 50:50, fetal bovine

serum (FBS), trypsin, and penicillin/streptomycin antibiotic cocktail were purchased from Corning® (Corning, NY). GlutaMAX™ and Neurobasal™ media were purchased from Gibco (Billings, MT). Thiazoly Blue Tetrazolium Bromide was purchased from VWR (Radnor, PA). B-27 100X supplement was purchased from Fisher Scientific (Waltham, MA). A lactate dehydrogenase (LDH) chemical assay kit, and all-trans retinoic acid were purchased from Cayman Chemical Company (Ann Arbor, MI). Potassium Chloride was purchased from Mallinckrodt (Staines-upon-Thames, United Kingdom). Brain derived neurotrophic factor (BDNF) was purchased from Prospec™ Bio (Rehovot, Israel).

Methods

Cell culture. SH-SY5Y cells were cultured based on instructions provided by American Type Culture Collection. Cells were grown in 10 cm plates and allowed to reach a confluency of 85% after approximately 5-6 days. After reaching 85% confluency cells were sub-cultured to new 10 cm plates at a 1:10 ratio. PBS was used to rinse cells before sub culturing and trypsin was used to uplift cells from plate. Cellular media was replaced every 3-4 days as needed.

Cellular differentiation. Cells were differentiated over an 11-day period using retinoic acid and brain derived neurotrophic factor.[35] Over the 11 days 3 different media compositions are used. The first was the base media used for general cell culturing for SH-SY5Y cells composed of DMEM/F12 media with 5% FBS and 1% penicillin/streptomycin (P/S). The second is stage 1 media which used DMEM/F12 50:50 as the base supplemented with 2.5% FBS, 1% P/S, and 10 µM all-trans retinoic acid. Lastly stage 2 media which used neurobasal media supplemented with 1X B-27, 20 mM KCl, 1% P/S, 2mM glutaMAX, and 50 ng/mL BDNF. Differentiation over 11 days was carried out as described in the literature.[35, 36]

PFAS exposure and cell collection. After the 11-day differentiation SH-SY5Y cells in 10 cm plates were exposed to 30 µM PFAS. PFAS treatments included PFOA, PFOS, PFDA, PFDS, 8:2 FTOH, and 8:2 FTS. Final treatment solutions included 1% MeOH. Treatments lasted 24 hours and were done in triplicate.

Viability assays. After day 11, treatments of PFAS in MeOH were added for final concentrations of 3, 10, 30, and 100 µM with 1% MeOH with a vehicle control of 1% MeOH. An additional treatment 10% Triton™ was added as a positive control for membrane permeabilization (n=5). Treatments lasted 24 hours.

MTT (3-(4,5-dimethylthiazol-2-yl)-2,5-diphenyltetrazolium bromide) assays were also performed. After a 24-hour PFAS treatment, cell plates were centrifuged at 200xg for 2 minutes at 24 ºC. Media was removed and 200 µL of 9% MTT in base media was added back. The plates were incubated at 37ºC under 5% CO_2 for 3 hours. After the plate was centrifuged a 150 µL portion of media was removed and 90 µL of DMSO was added back. Plates were then incubated at 37 ºC for 15 minutes and then mixed gently to dissolve formazan crystals. Absorbance was measured at 550 nm in a plate reader.

PFAS extraction and analysis. Frozen cell pellets were spiked with 1 mL of cold MeOH spiked with M4PFOS (deuterated standard used as an extraction control). Cell pellets were vortexed for 30 seconds and this was repeated 3 times for a total of 90 seconds. Cell pellets were sonicated at room temperature for 30 minutes and centrifuged at 14,000xg for 15 minutes. Supernatant was collected and dried down under a nitrogen stream. Extract was then resuspended in 970 µL of starting mobile phase (45% 5 mM ammonium acetate/55% methanol) spiked with M4PFOA (deuterated standard used as LC-MS/MS control). PFAS analysis was done via LC-MS/MS. Prior to LC-MS/MS analysis 8:2 FTOH was derivatized with dansyl chloride (please see supporting information for details).

LC-MS/MS analysis was done as described in detail in the SI. Briefly, a Raptor® C18 analytical column 2.7 µm particle size, 100 x 3 mm, was purchased from Restek (Centre County, PA). Separation for liquid chromatography tandem mass spectrometry (LC-MS/MS) analysis was performed using an Agilent® (Santa Clara, CA) 1200 series LC tower composed of a G13798 degasser, G1311A quaternary pump, G1367B high performance autosampler and G1330B autosampler thermostat. Mass analysis was done using a Thermo Scientific® (Waltham, MA) TSQ Quantum Ultra triple quadrupole MS equipped with a heated electrospray ionization source, operated under negative mode ionization. Details of the instrument parameters can be found in supporting information (Table S1).

RNA extraction, library preparation and sequencing. Frozen cell pellets were transported on dry ice to the University at Buffalo Genomics core and stored at -80ºC until analyzed. RNA was extracted using TriZol using Invitrogen protocols. Quality of RNA was assessed using Agilent's Fragment Analyzer and Qubit. RNA was then used to prepare an RNA library using an Illumina RiboZero Total Stranded RNA library prep kit. Libraries were pooled together at 10 nM with concentration being determined with a QuantaBio Universal qPCR reaction kit. The pooled library was sequenced using a NovaSeq6000 (PE100).

RNA-seq analysis. The obtained RNA sequences were evaluated using FastQC[37] and MultiQC[38] for quality control. Two samples were eliminated from the downstream analysis due to evidence of contamination. For five out of the six treatments, we have at least three samples, a sample was discarded each from the control and the FTOH treatment category, leaving two samples for the downstream analysis for each category. The two discarded samples were flagged as contamination due to their low number of successfully assigned alignments: for Control_3_S29 less than 14.2% of the reads were successfully mapped to the reference, while for FTOH_3_S47 a mere 14% of the total number of reads were successfully aligned. FastQC screen reports for the two samples confirmed that there are discrepancies with these samples either due to contamination or issues with the library preparation due to the presence of reads that produce multiple hits to multiple genomes. The RNA-seq reads were mapped to the human transcriptome reference (hg38) from Ensemble using hisat2[39] and quantified using featureCounts[40]. The differential expression analysis was carried out using DESeq2.[41] DESeq2 estimates the log fold-change of transcription for each gene using the Wald test of significance and performs multiple hypotheses correction on the raw read counts. DESeq2 can estimate dispersion with one 'degree of freedom,' calculated as the difference between the number of samples and the number of coefficients. In the context of our study after the removal of the two contaminants, there are four samples and two groups

(represented by two coefficients), thus, two 'degrees of freedom' are available. However, it is important to note that statistical power diminishes rapidly in this context, leading to a decreased sensitivity, thereby hindering the detection of smaller log-fold changes.[42] To determine the significantly differentially expressed genes we filtered our results for an p_{adj} of 0.05 (where the p_{adj} we refer to the multiple-hypotheses-corrected p-value).

The fastq RNA-seq data have been submitted to GEO and the project name will be provided once available.

Lipid extraction and analysis. Lipid extraction and sample preparation were carried out as we described previously.[43, 44] Samples were normalized based on their protein content and resuspended in spiked chloroform. C17:0 sphingomyelin, C^{13} oleic acid, C17:0 ceramide, C57:0 TAG, and C18:0/C18:0 phosphatidylcholine-d^{70} were used as internal standards. LC-MS-based lipid analysis analyses were carried out using an Agilent 1260 HPLC in tandem with an Agilent 6530 Jet Stream ESI-QToF-MS system as we described previously. Lipid species were targeted by extracting the corresponding *m/z* for each ion in MassHunter Qualitative Analysis software (v11). Peak areas for each ion were integrated and represented as abundance. Relative abundances used in heatmaps for the PFAS treatments (n=3) were normalized to the vehicle control by dividing the average abundance of a lipid species in the vehicle control by the individual abundances of each PFAS treatment sample.

RESULTS AND DISCUSSIONS

Effect of PFAS exposure on cell viability of differentiated SH-SY5Y cells. The SH-SY5Y cells were differentiated as we described previously[36] and treated with PFOA, PFOS, PFDA, PFDS, 8:2 FTOH, and 8:2 FTS for 24 hours at concentrations of 3, 10, 30, and 100 μM. Cell viability was assessed using MTT assays. None of the treatments induced reduction in cell viability (p-value > 0.05), except for 8:2 FTS, which induced a significant (p-value < 0.05) but modest cell death at 100 μM (~30%, **Figure 1**).

A challenge in PFAS exposure studies is mimicking the environmental PFAS exposure in a laboratory setting. Many forms of PFAS toxicity are chronic, taking place over years.[20] PFAS are commonly detected in human serum at low part per billion levels (ng/mL) or nanomolar concentrations,[45, 46] but do not exhibit toxicity in cultured cells up to 3~100 μM[14, 47, 48], consistent with our results. PFAS can reversibly bind to proteins which decreases bioavailability for uptake *in vitro*.[49] Based on the viability results we obtained, we selected 30 μM as the treatment concentration for follow-up investigations.

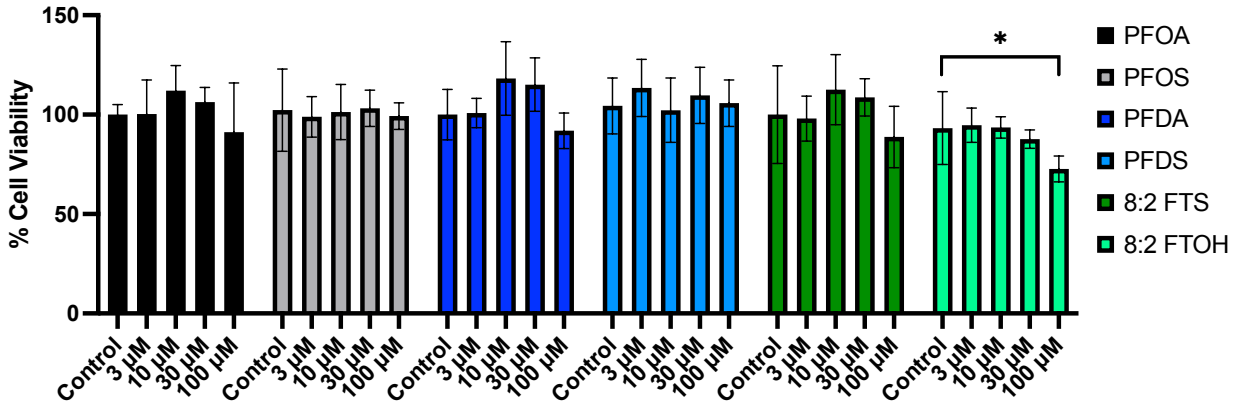

Figure 1: *MTT viability assay in SH-SY5Y cells with treatments of 3, 10, 30, and 100 µM PFOA, PFOS, PFDA, PFDS, 8:2 FTOH, and 8: FTS for 24-hours. 8:2 FTOH treatment at 100 µM showed a slight decrease in viability, which was statistically significant based on a paired t-test (* p-value < 0.05).*

PFAS uptake in differentiated SH-SY5Y cells. Total PFAS uptake in cells was determined via LC-MS/MS with single point standard addition. Treatments were carried out as described in the previous section. Cell pellets were collected, and protein contents were measured, followed by LC/MS/MS analysis (see SI, for detailed procedures, including the derivatization of 8:2 FTOH). **Table 1** shows the average uptake for each treatment. PFOA, PFOS, PFDA, PFDS, and 8:2 FTS treatments showed comparable uptake values at ~600 ng PFAS/mg protein. 8:2 FTOH, however, was quantified at ~12 ng PFAS/mg protein, considerably lower as compared to PFOA, PFOS, PFDA, PFDS and 8:2 FTS. The larger standard deviation observed is a result of biological variability between the three replicates. The lower cellular levels of 8:2 FTOH suggests either reduced uptake or metabolism of FTOHs, which have been reported *in vitro* and *in vivo*.[50, 51] A primary metabolite of 8:2 FTOH degradation is PFOA, as well as various fluorotelomer carboxylic acids.[52] A targeted LC/MS/MS analysis of PFOA, as a degradation product, showed no appreciable levels of PFOA in 8:2 FTOH treated cells, supporting that it is the reduced uptake of 8:2 FTOH as compared to other PFAS tested that causes low cellular levels. Overall, our data suggest that cellular uptake of PFAS increases with chain length, and fully fluorinated sulfonates exhibit the highest uptake while fluorotelomer alcohol shows the least cellular uptake in neuronal cells.

Table 1: *Uptake of PFAS in SH-SY5Y cells after a 30 µM exposure for 24 hrs (N=3) with a range defined by measured standard deviation (avg +/- 1 std).*

PFOA	526 +/- 259
PFOS	627 +/- 224
PFDA	522 +/- 190
PFDS	796 +/- 482

8:2 FTS	600 +/- 40
8:2 FTOH	9 +/- 7

Changes in gene expression in differentiated SH-SY5Y cells. To evaluate the impact of PFAS exposure in neuronal cells, we conducted a transcriptomics analysis to investigate pathways that are differently regulated after PFAS treatment. Differentiated SH-SH5Y cells were treated with PFOA, PFOS, PFDA, PFDS, 8:2 FTOH, and 8:2 FTS at 30 μM. Cells were collected as described in the methods section. After mRNA extraction (n=3 for each condition), the mRNA content was sequenced using Illumina sequencing. Gene expression in treatments were compared to a control and was calculated as $\log_2$ fold change (Log_2 FC). Genes which showed differences in expression levels between treatment and control, and had a $p_{adj} < 0.05$, were compiled in a list for further statistical analysis and Gene Ontology (GO) gene enrichment.

Figure 2 represents data for the total pool of differently expressed genes impacted by all six treatments as compared to the control, and the distribution of the number of genes affected per treatment. Each bar represents an individual treatment, and colors represent genes from the pool affected by the specific PFAS treatment. Gray, blue, and red represent differentially expressed genes ($p_{adj} < 0.05$) with various fold change (FC) thresholds: gray represents $\log_2$FC <[0.5], blue represents $\log_2$FC [0.5-.99], and red represents $\log_2$FC >[1]). White sections correspond to genes that are not affected by the given treatment. This analysis resulted in 721 unique genes that were impacted across the six treatments combined. PFOA treatment affected the largest number of genes out of the six treatments, significantly changing the expression of 584 genes ($p_{adj} < 0.05$). In comparison, the remaining 5 PFAS chemicals each only impacted approximately 100 genes ($p_{adj} < 0.05$, PFOS,102 genes; PFDS, 106 genes; PFDA, 147 genes; 8:2 FTS, 100 genes; and 8:2 FTOH, 67 genes). While PFOA affected the greatest number of genes, the magnitude of the changes were low (log2FC < 0.5). In contrast, PFOS affected a smaller number of genes but at much higher level ($\log_2$FC > 1) (**Figure 2**, see **Table S2** for a complete list of genes separated by treatment group and sorted by $\log_2$FC).

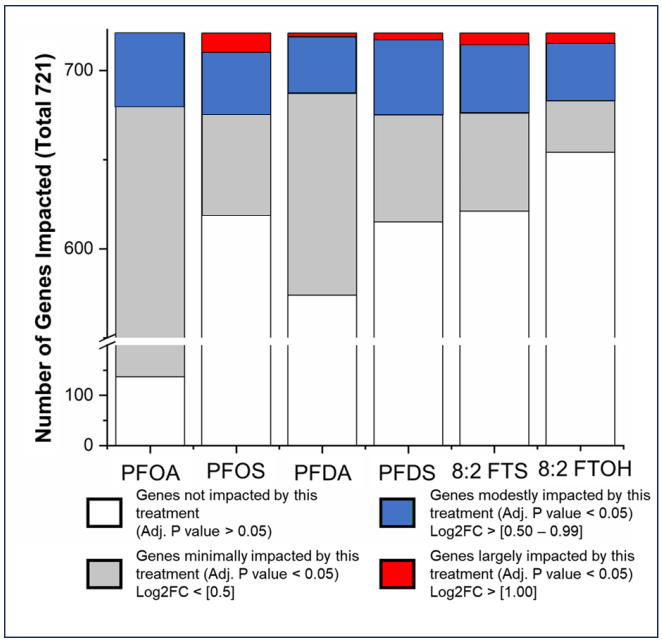

Figure 2: *Distribution of log_2FC observed for gene expression in SH-SY5Y cells after exposure to six different PFAS species. Log2FC > [0.5] were selected. Log_2FC of > [1] was chosen to represent genes that were doubled or halved in expression and comprised less than 1% of the genes impacted by the PFAS treatments.*

To visualize differentially expressed genes that are common between different treatment groups, an upset plot was generated. This plot groups impacted genes by the number of overlapping treatments (**Figure 3**). Among the 721 differentially expressed genes, 425 were unique to PFOA treatment. Treatments with other PFAS uniquely affected 13 to 36 genes, while 193 genes showed differential expression under combinations of different PFAS treatments. PFDA and PFOA treatments affected the expression of 53 common genes, possibly due to the carboxylate headgroup they share. Another noteworthy observation was that 11 genes (10 protein coding and one RNA coding) were differentially regulated in all six treatments (**Figure 3**).

Overall, these results point towards a few important observations. First, among the PFAS tested, PFOA induced the highest number of changes in gene expression, suggesting that PFOA is more potent in perturbating cellular homeostasis than other PFAS. Second, PFDA and PFOA, which are both carboxylated, had the highest overlap among differentially expressed genes, suggesting that the type of head group may significantly influences cellular effects of PFAS. Finally, our results revealed 11 genes as potential biomarkers of PFAS exposure, as their expressions were significantly affected by all six PFAS treatments.

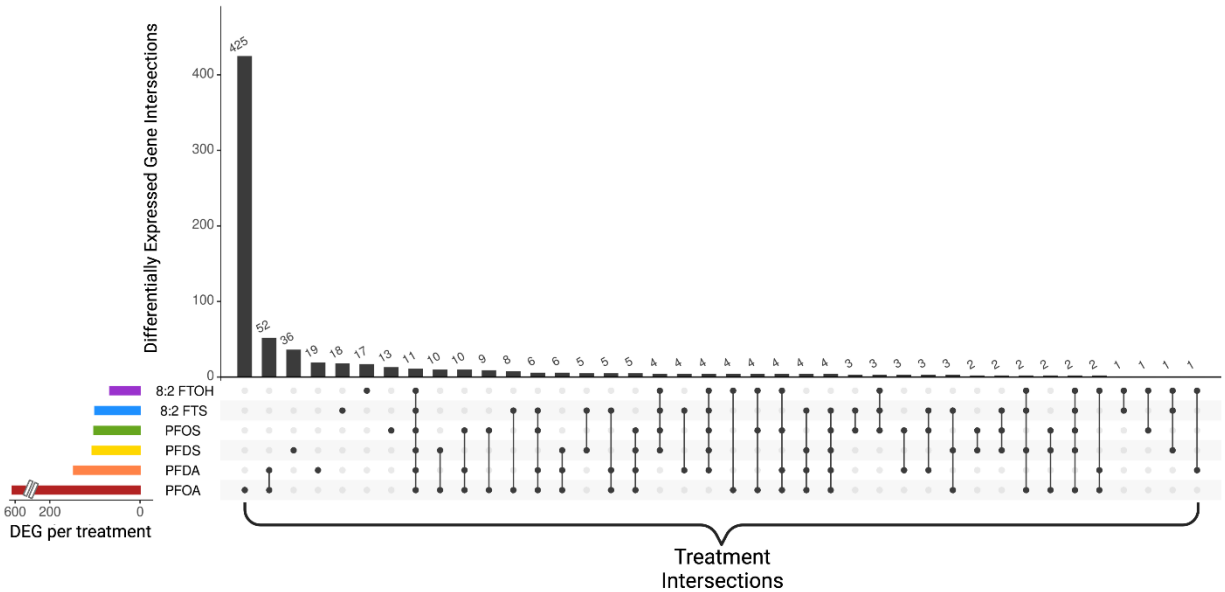

Figure 3: *An upset plot to visualize the grouping of genes that overlap in multiple treatments. Treatment intersections are defined by treatments that can be grouped by commonality and, in this context, overlapping differentially expressed genes. Differentially expressed genes (DEGs) are genes that were found to have log2FC > 0 and log2FC < 0 after a PFAS treatment compared to a control (*$p_{adj} < 0.05$*).*

Potential markers of PFAS exposure. The Organization for Economic Cooperation and Development (OECD) contains a database of 4700 unique PFAS chemicals[53], and about 6% (256 PFAS) are commercial products, byproducts, or known degradation materials.[5] It is therefore important to develop assays to assess exposure to PFAS when direct PFAS measurements from tissue are not feasible. Analysis of peripheral markers of PFAS exposure could be a powerful tool to assess exposure and risk to a potential disease progression.

Recent studies demonstrated that changes in protein expression related to neurodegenerative diseases can be measured in peripheral body fluids such as blood and saliva.[54, 55] It has also been shown that damage to the BBB can lead to release of proteins from the brain to the blood[56]. Further, PFAS can disrupt the BBB through oxidative stress and may also lead to this leakage.[25]

We identified 10 protein coding genes that were impacted by all six treatments using transcriptomics. These are *Transmembrane protein 106B* (TMEM106B), *transmembrane p24 trafficking protein 7* (TMED7), *T-box 3* (TBX3), *mesencephalic astrocyte derived neurotrophic factor* (MANF), *pyruvate dehydrogenase kinase 1* (PDK1), *BCL2 interacting protein 3* (BNIP3), *isoleucyl-tRNA synthetase 1* (IARS3), *mitotic spindle organizing protein 1* (MZT1), *thioredoxin interacting protein* (TXNIP) and *H4 clustered histone 13* (HIST1H4L). Each gene was differentially regulated in the same direction (i.e., upregulation or downregulation, **Figure 4)**. Such uniform response indicates that these genes could be used as a potential biomarker(s) to assess

PFAS exposure, independently or combined. Future efforts investigating the regulation of these changes in other PFAS are warranted to explore these changes as biomarkers of PFAS exposure.

Potential adverse effects of PFAS exposure assessed by changes in gene expression. We used several strategies to investigate the implications of the PFAS-induced differential expression. To focus on biological relevance, we considered the effect size of gene expression differentiation in this analysis. Thus, in addition to the ten genes that are impacted by all treatments (**Figure 4**, red arrow), we focused on the genes that showed at least two-fold change in at least three treatments (**Figure 4**, blue arrow). The resulting list constituted less than 1% of the total genes impacted.

Multiple genes that were affected in this resulting list have been implicated to various pathologies. These include BNIP3[57], HIST1H4L[58], TBX3[59], MANF[60] and TXNIP[61] (observed in all six treatments), early growth response factor 1 (*EGR1*)[62], solute carrier family 7 member 11 (*SLC7A11*)[59] and tolloid-like protein 2 (*TLL2*)[63] (observed in 5 treatments), niban apoptosis regulator 1 (*NIBAN1*)[64] and fos proto-oncogene (*FOS*)[65] (observed in 3 treatments). Importantly, MANF and TXNIP have previously been implicated in neuronal health. MANF, which was downregulated in all treatments, is an important protein for survival of neuronal cells, and evidence in rats has suggested that MANF can reverse symptoms of neurodegenerative diseases.[60] TXNIP, on the other hand, was upregulated in all treatments, and has been linked to oxidative stress resulting in neuronal death and neurodegenerative diseases.[61]

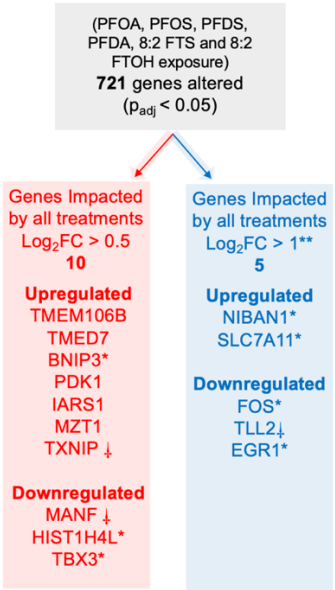

Figure 4: *Fifteen notable genes which were impacted after exposure to PFOS, PFOA, PFDS, PFDA, 8:2 FTS, 8:2 FTOH. Of 721 genes that were differently ($p_{adj} < 0.05$), 10 genes were common to all treatments (red arrow). 5 genes that were regulated in at least three treatments had log_2FC >1. *Genes that, when dysregulated, have been linked to a cancerous pathology. ⸸Genes that, when dysregulated, have been linked to neurodegenerative disorders.**Genes in this list were impacted in at least three out of six treatments.*

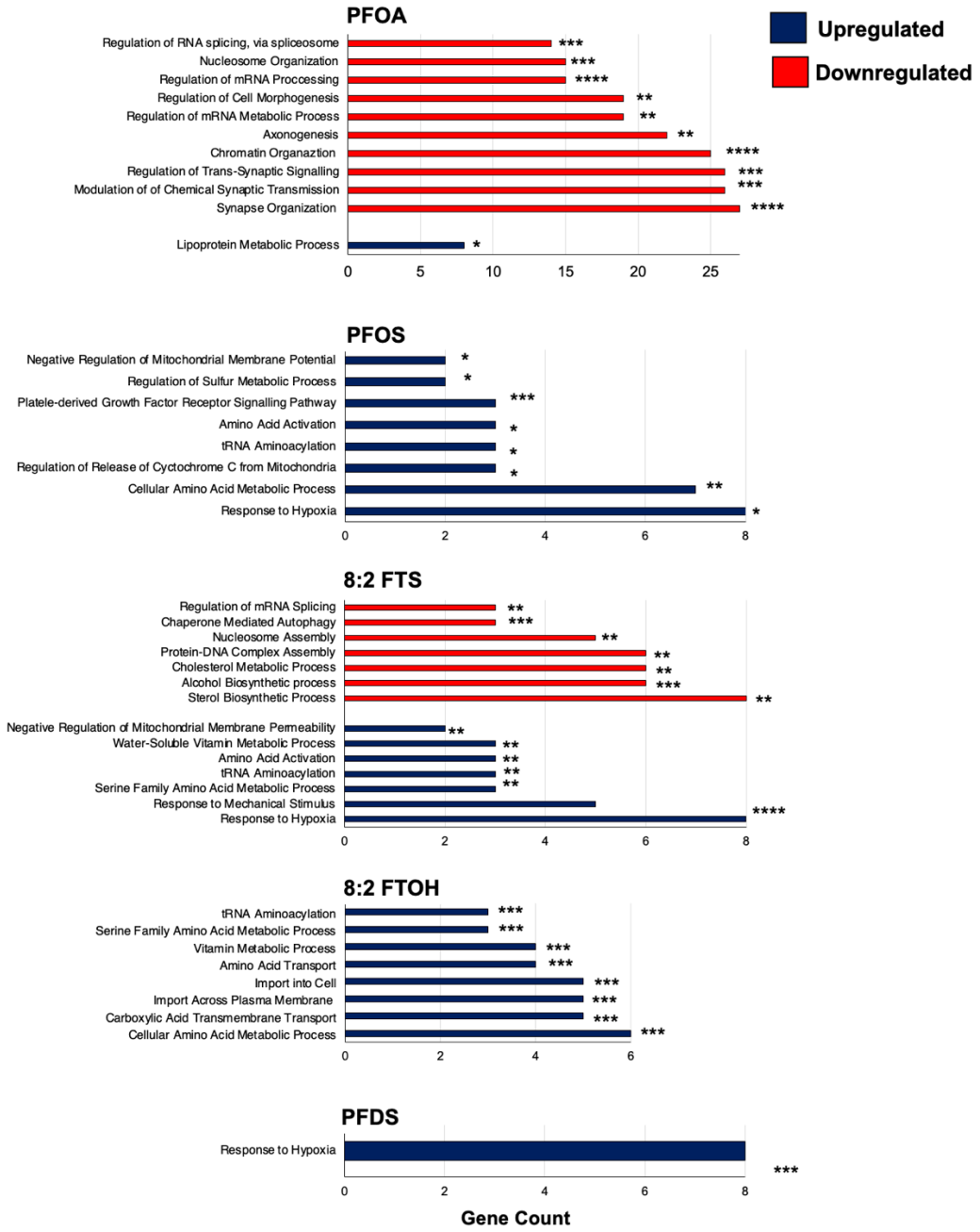

Figure 5: *GO gene enrichment analysis for discovering potential biological pathways affected by PFOA, PFOS, PFDS, 8:2 FTS, and 8:2 FTOH treatments. Genes used for this analysis were genes impacted by each treatment with log2FC>0.5 (control vs treatment) with* $p_{adj} < 0.05$*. The multiple hypothesis corrected p-values are shown in the figure:* $p_{adj} < 0.05$*). ***\

Gene enrichment analysis suggest PFOA can affect neurodevelopment and neurotoxicity. To identify biological processes that are impacted by PFAS exposure, we conducted gene enrichment analysis (**Figure 5** and **Table S3**). A total of 34 biological processes were found to be significantly enriched ($p_{adj} < 0.05$) among differentially expressed genes. Among these genes, the ones downregulated by PFOA treatment are enriched for neuronal processes, including the development of axons from neurons to deliver action potentials, regulation of trans-synaptic signaling, modulation of chemical synaptic signaling, and synapse organization. This enrichment may suggest that PFOA impacts the neuronal networks in SH-SY5Y cells. Consistent with this observations, studies showed that PFOA treatment led to 20-25% reduction in neurite outgrowth[66], decreased neurite density and altered nucleolus and mitochondria in neuronal cells[67]. Similarly, PFOA exposure in mice led to overexpression of brain-development related proteins and another legacy PFAS, PFOS, affected learning in zebrafish embryos.[68] Our results confirm the emerging idea that PFAS, and PFOA in particular, may affect neuronal development and function, with major implications to neurological disorders.

Hypoxia- and tRNA aminoacylation-related genes are enriched in differential expression after PFAS treatment. While the mechanisms are unknown, PFAS exposure has been shown to induce hypoxic state, adversely affect cellular energy production and increase production of ROS in neuronal cells.[75] We found hypoxia-related genes to be significantly enriched after treatment of differentiated SH-SY5Y cell with PFOS, PFDS and 8:2 FTS, sulfate-containing species among the PFAS we tested. These genes include adenylate kinase family (*AK4*), BNIP3, and pyruvate dehydrogenase kinase 1 (*PDK1*), which are linked to hypoxia inducible factor 1 subunit alpha (*HIF-1α*) functioning. Vascular endothelial growth factor A (*VEGFA*)[69], stanniocalcin-2 (*STC2*)[70], phorbol-12-myristate-13-acetate-induced protein 1 (*PMAIP1*)[71], hexokinase 2 (*HK2*)[72], *SLC2A1*[73], and DNA damage inducible transcript 4 (*DDIT4*)[74] were also upregulated in at least one PFAS treatment. Our results suggest that sulfonate containing PFAS have a higher propensity to induced hypoxia signaling as compared to their counterparts, with different headgroups.

Finally, we observed that several genes involved in tRNA aminoacylation, including cysteinyl-tRNA synthetase 1 (*CARS1*), aspartyl-tRNA synthetase 1 (*DARS1*), and *IARS1* were upregulated with PFOS, 8:2 FTOH, and 8:2 FTS treatment. These enzymes are responsible for the addition of cysteine, aspartic acid, and isoleucine to tRNA molecules necessary for protein synthesis, respectively, and are upregulated in the pro-proliferative state of cancer cells.[76] Interestingly, PFOS, 8:2 FTOH, and 8:2 FTS treatments also result in upregulating amino acid uptake/transport and metabolism-related processes, which have been linked to the increased energy requirement in cells.[77,78] While further investigations are needed to study the effects of PFAS on protein synthesis and cellular metabolism, these results suggest their significant effects on critical processes involved cellular homeostasis.

PFAS treatment impact lipidome of differentiated SH-SY5Y cells. Our results show that PFAS induce different changes at the transcript level and that different biological processes are enriched in these observations based on their chemical structure. To investigate the effects of PFAS in this context using a different end point assessment, we focused PFDA, PFDS, 8:2 FTOH and 8:2 FTS as PFAS representing different head groups and degree of fluorination and studied the changes that they induce at the cellular lipidome. Following a similar treatment protocol described above

we treated differentiated cells with these PFAS at 30 μM and analyzed the changes in the cellular lipidome compared to control group (see methods for details for sample preparation and lipid analysis). We targeted abundant lipid classes, including fatty acids, phosphatidylserines, phosphatidylcholines, diacylglycerols, and triacylglycerols, ceramides, and sphingomyelins with different acyl chain lengths and degrees of unsaturation. Fatty acids significantly accumulated (i.e., ~1.5-2.7-fold changes, $p < 0.05$) in cells treated with PFDA, PFDS and 8:2 FTS (**Figure 6**), while phospholipids and diacylglycerols remained unchanged. Interestingly, only 8:2 FTOH treatment caused depletions in several TAG species ($p < 0.05$). Sphingolipids also exhibited PFAS-specific changes where we observed accumulations of a few ceramide species (i.e., ~1.2-1.3-fold) and sphingomyelins (~1.4-1.7 fold) treated with PFDA and 8:2 FTS (**Figure 6**). Overall, these results support our observation from transcriptomics analysis that that PFAS have varying effects at the cellular level, which might affect their negative health effects.

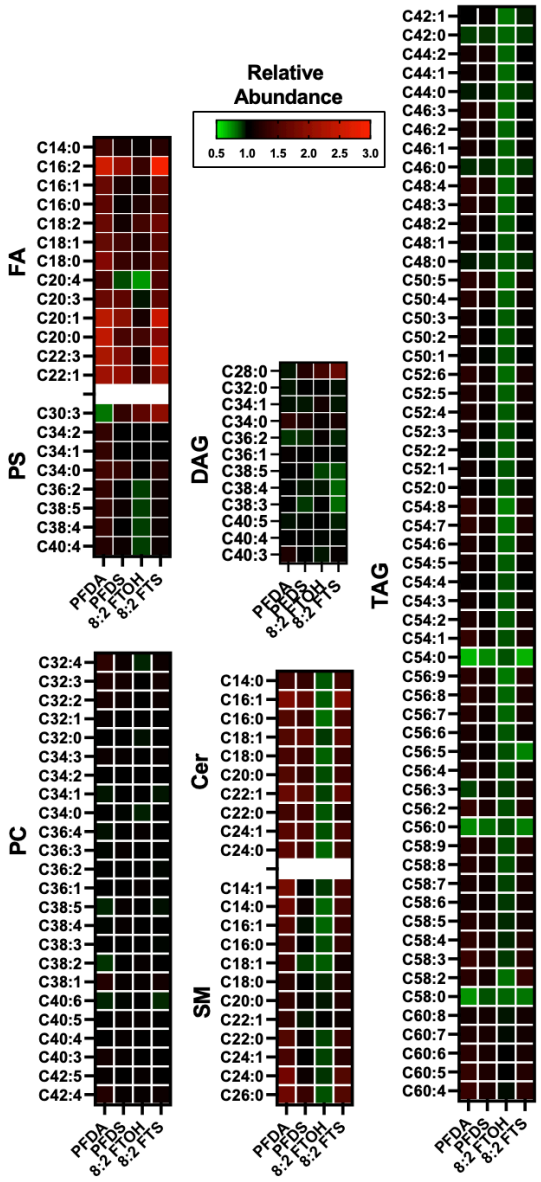

Figure 6. Targeted lipidomics highlight changes in fatty acids and glycerolipids in response to PFAS treatment in differentiated SH-SY5Y cells. Targeted lipids include fatty acids (FA), phosphatidylserine (PS), phosphatidylcholine (PC), diacylglycerols (DAG), triacylglycerols (TAG), ceramides (Cer), and sphingomyelin (SM). The red-to-green heat map shows the fold changes calculated by dividing the abundances of each PFAS treatment by the average abundance of the MeOH control. *p-value ≤ 0.05; **p-value ≤ 0.01.

CONCLUSIONS

In this study, differentiated SH-SY5Y cells were used as a model for human neurons to assess the transcriptomic impact of PFOS, PFOA, PFDS, PFDA, 8:2 FTS and 8:2 FTOH, which have all been previously detected in human and animal brain tissues. We observed similar cellular uptake levels of PFOS, PFOA, PFDS, and 8:2 FTS, while cellular 8:2 FTOH levels were much lower. The fact that 8:2 FTOH is the only neutral species tested suggest that PFAS uptake is strongly influenced by the nature of the headgroup. Using transcriptomics, we identified hundreds of genes affected by PFAS exposure. PFOA treatment impacted 3-6 times more genes (~600) than the other treatments. PFOA-affected genes are enriched for biological processes related to neurite growth, neurite organization, and action potential, indicating potential links to neurodegenerative diseases. Among the other PFAS we tested, sulfate head group containing PFAS and fluorotelomeric PFAS affected genes enriched in biological processes related to response to hypoxic state and cellular metabolism, respectively. Supporting these observations that PFAS exhibit structures-specific effects, PFDA, PFDS, 8:2 FTS and 8:2 FTOH induced various changes in the cellular lipidome, PFDA, PFDS and 8:2 FTS affecting fatty acid levels, and 8:2 FTOH causing depletions in triacylglycerols. It is important to note that, while 8:2 FTOH uptake to 50-60-fold less as compared to the other PFAS we tested, it induces changes at similar extent to other PFAS, indicating higher propensity of 8:2 FTOH to perturb cellular homeostasis compared to its carbonylated and sulfonated counterparts. Overall, results from this study provide valuable insight to the biological mechanisms through which PFAS affect neuronal biology and health. Future work will focus on understanding the mechanism of how PFAS induce these changes and potential links to different disease models.

Acknowledgements
We gratefully acknowledge the support from the National Science Foundation (CBET-2112201). Any opinions, findings, conclusions, or recommendations expressed in this publication are those of the author(s) and do not necessarily reflect the view of the NSF.

References:

(1) Lewis, R. C.; Johns, L. E.; Meeker, J. D. Serum biomarkers of exposure to perfluoroalkyl substances in relation to serum testosterone and measures of thyroid function among adults and adolescents from nhanes 2011–2012. *International Journal of Environmental Research and Public Health* **2015**, *12* (6), 6098-6114. DOI: 10.3390/ijerph120606098.
(2) Shu, H.; Lindh, C. H.; Wikström, S.; Bornehag, C.-G. Temporal trends and predictors of perfluoroalkyl substances serum levels in Swedish pregnant women in the SELMA study. *PLOS ONE* **2019**, *13* (12).
(3) Hurley, S.; Goldberg, D.; Wang, M.; Park, J.-S.; Petreas, M.; Bernstein, L.; Anton-Culver, H.; Nelson, D. O.; Reynolds, P. Time Trends in Per- and Polyfluoroalkyl Substances (PFASs) in California Women: Declining Serum Levels, 2011–2015. *Environmental Science & Technology* **2018**, *52* (1), 277-287. DOI: 10.1021/acs.est.7b04650.
(4) Multi-Industry Per- and Polyfluoroalkyl Substances (PFAS) Study – 2021 Preliminary Report. Agency, U. S. E. P., Ed.; 1200 Pennsylvania Avenue, NW Washington, DC 20460, 2021.
(5) Buck, R. C.; Korzeniowski, S. H.; Laganis, E.; Adamsky, F. Identification and classification of commercially relevant per- and poly-fluoroalkyl substances (PFAS). *Integrated Environmental Assessment and Management* **2021**, *17* (5), 1045-1055, https://doi.org/10.1002/ieam.4450. DOI: https://doi.org/10.1002/ieam.4450 (acccessed 2023/03/28).
(6) Buck, R. C.; Franklin, J.; Berger, U.; Conder, J. M.; Cousins, I. T.; de Voogt, P.; Jensen, A. A.; Kannan, K.; Mabury, S. A.; van Leeuwen, S. P. Perfluoroalkyl and polyfluoroalkyl substances in the environment: terminology, classification, and origins. *Integrated Environmental Assessment and Management* **2011**, *7* (4), 513-541. DOI: 10.1002/ieam.258 From NLM.
(7) Shahsavari, E.; Rouch, D.; Khudur, L. S.; Thomas, D.; Aburto-Medina, A.; Ball, A. S. Challenges and current wtatus of the biological treatment of PFAS-contaminated soils. *Frontiers in Bioengineering and Biotechnology* **2020**, *8*, 602040. DOI: 10.3389/fbioe.2020.602040 From NLM.
(8) Kelly, B. C.; Ikonomou, M. G.; Blair, J. D.; Surridge, B.; Hoover, D.; Grace, R.; Gobas, F. A. P. C. perfluoroalkyl contaminants in an arctic marine food web: trophic magnification and wildlife exposure. *Environmental Science & Technology* **2009**, *43* (11), 4037-4043. DOI: 10.1021/es9003894.
(9) Bartels, J. L.; Aweda, T. A.; Rosenberg, A. J.; Lunderberg, D. M.; Peaslee, G. F.; Lapi, S. E. Radiosynthesis and biological distribution of 18F-labeled perfluorinated alkyl substances. *Environmental Science & Technology Letters* **2017**, *4* (6), 211-215. DOI: 10.1021/acs.estlett.7b00042.
(10) Nicole, W. Breaking It down: estimating short-chain PFAS half-lives in a human population. *Environmental Health Perspectives* **2020**, *128* (11), 114002. DOI: 10.1289/ehp7853 From NLM.
(11) Li, Y.; Andersson, A.; Xu, Y.; Pineda, D.; Nilsson, C. A.; Lindh, C. H.; Jakobsson, K.; Fletcher, T. Determinants of serum half-lives for linear and branched perfluoroalkyl substances after long-term high exposure—A study in Ronneby, Sweden. *Environment International* **2022**, *163*, 107198. DOI: https://doi.org/10.1016/j.envint.2022.107198.
(12) Lucas, K.; Gaines, L. G. T.; Paris-Davila, T.; Nylander-French, L. A. Occupational exposure and serum levels of per- and polyfluoroalkyl substances (PFAS): A review. *American*

Journal of Industrial Medicine **2023**, *66* (5), 379-392, https://doi.org/10.1002/ajim.23454. DOI: https://doi.org/10.1002/ajim.23454 (acccessed 2023/05/09).
(13) Pérez, F.; Nadal, M.; Navarro-Ortega, A.; Fàbrega, F.; Domingo, J. L.; Barceló, D.; Farré, M. Accumulation of perfluoroalkyl substances in human tissues. *Environment International* **2013**, *59*, 354-362. DOI: https://doi.org/10.1016/j.envint.2013.06.004.
(14) Running, L.; Atilla-Gokcumen, G. E.; Aga, D. S. Development of a liquid chromatography–mass spectrometry-based In vitro assay to assess changes in steroid hormones due to exposure to per- and polyfluoroalkyl substances. *Chemical Research in Toxicology* **2022**, *35* (7), 1277-1288. DOI: 10.1021/acs.chemrestox.2c00116.
(15) Ahmed, K. E. M.; Frøysa, H. G.; Karlsen, O. A.; Blaser, N.; Zimmer, K. E.; Berntsen, H. F.; Verhaegen, S.; Ropstad, E.; Kellmann, R.; Goksøyr, A. Effects of defined mixtures of POPs and endocrine disruptors on the steroid metabolome of the human H295R adrenocortical cell line. *Chemosphere* **2019**, *218*, 328-339. DOI: 10.1016/j.chemosphere.2018.11.057 From NLM.
(16) Mokra, K. Endocrine disruptor potential of short- and long-chain perfluoroalkyl substances (PFASs)-A synthesis of current knowledge with proposal of molecular mechanism. *International Journal of Molecular Sciences* **2021**, *22* (4). DOI: 10.3390/ijms22042148 From NLM.
(17) Louisse, J.; Fragki, S.; Rijkers, D.; Janssen, A.; van Dijk, B.; Leenders, L.; Staats, M.; Bokkers, B.; Zeilmaker, M.; Piersma, A.; et al. Determination of in vitro hepatotoxic potencies of a series of perfluoroalkyl substances (PFASs) based on gene expression changes in HepaRG liver cells. *Archives of Toxicology* **2023**, *97* (4), 1113-1131. DOI: 10.1007/s00204-023-03450-2.
(18) Liu, Y.; Lin, N.; Dai, C.; Xu, J.; Zhang, Y.; Xu, M.; Wang, F.; Li, Y.; Chen, D. Occurrence and distribution of per- and polyfluoroalkyl substances (PFASs) in human livers with liver cancer. *Environmental Research* **2021**, *202*, 111775. DOI: https://doi.org/10.1016/j.envres.2021.111775.
(19) Costello, E.; Rock, S.; Stratakis, N.; Eckel Sandrah, P.; Walker Douglas, I.; Valvi, D.; Cserbik, D.; Jenkins, T.; Xanthakos Stavra, A.; Kohli, R.; et al. Exposure to per- and polyfluoroalkyl substances and markers of liver injury: A systematic review and meta-analysis. *Environmental Health Perspectives 130* (4), 046001. DOI: 10.1289/EHP10092 (acccessed 2023/05/09).
(20) Fenton, S. E.; Ducatman, A.; Boobis, A.; DeWitt, J. C.; Lau, C.; Ng, C.; Smith, J. S.; Roberts, S. M. Per- and polyfluoroalkyl substance toxicity and human health review: current state of knowledge and strategies for informing future research. *Environmental Toxicology and Chemistry* **2021**, *40* (3), 606-630, https://doi.org/10.1002/etc.4890. DOI: https://doi.org/10.1002/etc.4890 (acccessed 2023/05/11).
(21) Boyd, R. I.; Ahmad, S.; Singh, R.; Fazal, Z.; Prins, G. S.; Madak Erdogan, Z.; Irudayaraj, J.; Spinella, M. J. Toward a mechanistic understanding of poly- and perfluoroalkylated substances and cancer. *Cancers* **2022**, *14* (12). DOI: 10.3390/cancers14122919.
(22) Kimura, O.; Kondo, Y.; Shimosegawa, T. Ppar could contribute to the pathogenesis of hepatocellular carcinoma. *PPAR Research* **2012**, *2012*, 574180. DOI: 10.1155/2012/574180 From NLM.
(23) Wang, J.; Pan, Y.; Cui, Q.; Yao, B.; Wang, J.; Dai, J. Penetration of pfass across the blood cerebrospinal fluid barrier and its determinants in humans. *Environmental Science & Technology* **2018**, *52* (22), 13553-13561. DOI: 10.1021/acs.est.8b04550 From NLM.
(24) Harada, K. H.; Hashida, S.; Kaneko, T.; Takenaka, K.; Minata, M.; Inoue, K.; Saito, N.; Koizumi, A. Biliary excretion and cerebrospinal fluid partition of perfluorooctanoate and

perfluorooctane sulfonate in humans. *Environmental Toxicology and Pharmacology* **2007**, *24* (2), 134-139. DOI: 10.1016/j.etap.2007.04.003 From NLM.
(25) Cao, Y.; Ng, C. A. Absorption, distribution, and toxicity of per- and polyfluoroalkyl substances (PFAS) in the brain: a review. *Environmental Science. Processes & Impacts* **2021**.
(26) Di Nisio, A.; Pannella, M.; Vogiatzis, S.; Sut, S.; Dall'Acqua, S.; Rocca, M. S.; Antonini, A.; Porzionato, A.; De Caro, R.; Bortolozzi, M.; et al. Impairment of human dopaminergic neurons at different developmental stages by perfluoro-octanoic acid (PFOA) and differential human brain areas accumulation of perfluoroalkyl chemicals. *Environment International* **2022**, *158*, 106982. DOI: https://doi.org/10.1016/j.envint.2021.106982.
(27) Zhang, L.; Ren, X.-M.; Guo, L.-H. Structure-based investigation on the interaction of perfluorinated compounds with human liver fatty acid binding protein. *Environmental Science & Technology* **2013**, *47* (19), 11293-11301. DOI: 10.1021/es4026722.
(28) Louisse, J.; Dellafiora, L.; van den Heuvel, J. J. M. W.; Rijkers, D.; Leenders, L.; Dorne, J.-L. C. M.; Punt, A.; Russel, F. G. M.; Koenderink, J. B. Perfluoroalkyl substances (PFASs) are substrates of the renal human organic anion transporter 4 (OAT4). *Archives of Toxicology* **2023**, *97* (3), 685-696. DOI: 10.1007/s00204-022-03428-6.
(29) Yu, Y.; Wang, C.; Zhang, X.; Zhu, J.; Wang, L.; Ji, M.; Zhang, Z.; Ji, X.-M.; Wang, S.-L. Perfluorooctane sulfonate disrupts the blood brain barrier through the crosstalk between endothelial cells and astrocytes in mice. *Environmental Pollution* **2020**, *256*, 113429. DOI: https://doi.org/10.1016/j.envpol.2019.113429.
(30) Brown-Leung, J. M.; Cannon, J. R. Neurotransmission targets of per- and polyfluoroalkyl substance neurotoxicity: Mechanisms and potential implications for adverse neurological outcomes. *Chemical Research in Toxicology* **2022**, *35* (8), 1312-1333. DOI: 10.1021/acs.chemrestox.2c00072.
(31) Mastrantonio, M.; Bai, E.; Uccelli, R.; Cordiano, V.; Screpanti, A.; Crosignani, P. Drinking water contamination from perfluoroalkyl substances (PFAS): an ecological mortality study in the Veneto Region, Italy. *European Journal of Public Health* **2018**, *28* (1), 180-185. DOI: 10.1093/eurpub/ckx066 (acccessed 5/11/2023).
(32) Anderko, L.; Pennea, E. Exposures to per-and polyfluoroalkyl substances (PFAS): Potential risks to reproductive and children's health. *Current Problems in Pediatric and Adolescent Health Care* **2020**, *50* (2), 100760. DOI: https://doi.org/10.1016/j.cppeds.2020.100760.
(33) Jurewicz, J.; Polańska, K.; Hanke, W. Chemical exposure early in life and the neurodevelopment of children--an overview of current epidemiological evidence. *Annals of Agricultural and Environmental Medicine* **2013**, *20* (3), 465-486. From NLM.
(34) Vuong, A. M.; Webster, G. M.; Yolton, K.; Calafat, A. M.; Muckle, G.; Lanphear, B. P.; Chen, A. Prenatal exposure to per- and polyfluoroalkyl substances (PFAS) and neurobehavior in US children through 8 years of age: The HOME study. *Environmental Research* **2021**, *195*, 110825. DOI: https://doi.org/10.1016/j.envres.2021.110825.
(35) Dravid, A.; Raos, B.; Svirskis, D.; O'Carroll, S. J. Optimised techniques for high-throughput screening of differentiated SH-SY5Y cells and application for neurite outgrowth assays. *Scientific Reports* **2021**, *11* (1), 23935. DOI: 10.1038/s41598-021-03442-1.
(36) Camdzic, M.; Aga, D. S.; Atilla-Gokcumen, G. E. Cellular lipidome changes during retinoic acid (ra)-induced differentiation in sh-sy5y cells: A comprehensive in vitro model for assessing neurotoxicity of contaminants. *Environment & Health* **2023**, *1* (2), 110-120. DOI: 10.1021/envhealth.3c00022.

(37) Wingett, S. W.; Andrews, S. FastQ Screen: A tool for multi-genome mapping and quality control. *F1000Res* **2018**, *7*, 1338. DOI: 10.12688/f1000research.15931.2 From NLM.
(38) Ewels, P.; Magnusson, M.; Lundin, S.; Käller, M. MultiQC: summarize analysis results for multiple tools and samples in a single report. *Bioinformatics* **2016**, *32* (19), 3047-3048. DOI: 10.1093/bioinformatics/btw354 (acccessed 5/25/2023).
(39) Kim, D.; Paggi, J. M.; Park, C.; Bennett, C.; Salzberg, S. L. Graph-based genome alignment and genotyping with HISAT2 and HISAT-genotype. *Nature Biotechnology* **2019**, *37* (8), 907-915. DOI: 10.1038/s41587-019-0201-4.
(40) Liao, Y.; Smyth, G. K.; Shi, W. featureCounts: an efficient general purpose program for assigning sequence reads to genomic features. *Bioinformatics* **2014**, *30* (7), 923-930. DOI: 10.1093/bioinformatics/btt656 (acccessed 5/25/2023).
(41) Love, M. I.; Huber, W.; Anders, S. Moderated estimation of fold change and dispersion for RNA-seq data with DESeq2. *Genome Biology* **2014**, *15* (12), 550. DOI: 10.1186/s13059-014-0550-8.
(42) Schurch, N. J.; Schofield, P.; Gierliński, M.; Cole, C.; Sherstnev, A.; Singh, V.; Wrobel, N.; Gharbi, K.; Simpson, G. G.; Owen-Hughes, T.; et al. How many biological replicates are needed in an RNA-seq experiment and which differential expression tool should you use? *Rna* **2016**, *22* (6), 839-851. DOI: 10.1261/rna.053959.115 From NLM.
(43) Millner, A.; Lizardo, D. Y.; Atilla-Gokcumen, G. E. Untargeted Lipidomics Highlight the Depletion of Deoxyceramides during Therapy-Induced Senescence. *Proteomics* **2020**, *20* (10), e2000013. DOI: 10.1002/pmic.202000013 From NLM Medline.
(44) Li, N.; Lizardo, D. Y.; Atilla-Gokcumen, G. E. Specific Triacylglycerols Accumulate via Increased Lipogenesis During 5-FU-Induced Apoptosis. *ACS Chem Biol* **2016**, *11* (9), 2583-2587. DOI: 10.1021/acschembio.6b00410 From NLM Medline.
(45) Jian, J. M.; Chen, D.; Han, F. J.; Guo, Y.; Zeng, L.; Lu, X.; Wang, F. A short review on human exposure to and tissue distribution of per- and polyfluoroalkyl substances (PFASs). *Science of the Total Envirorment* **2018**, *636*, 1058-1069. DOI: 10.1016/j.scitotenv.2018.04.380 From NLM.
(46) Pitter, G.; Da Re, F.; Canova, C.; Barbieri, G.; Zare Jeddi, M.; Daprà, F.; Manea, F.; Zolin, R.; Bettega, A. M.; Stopazzolo, G.; et al. Serum levels of perfluoroalkyl substances (pfas) in adolescents and young adults exposed to contaminated drinking water in the veneto region, italy: A cross-sectional study based on a health surveillance program. *Environmental Health Perspectives* **2020**, *128* (2), 27007. DOI: 10.1289/ehp5337 From NLM.
(47) Behr, A. C.; Lichtenstein, D.; Braeuning, A.; Lampen, A.; Buhrke, T. Perfluoroalkylated substances (PFAS) affect neither estrogen and androgen receptor activity nor steroidogenesis in human cells in vitro. *Toxicology Letters* **2018**, *291*, 51-60. DOI: 10.1016/j.toxlet.2018.03.029 From NLM.
(48) Solan, M. E.; Senthilkumar, S.; Aquino, G. V.; Bruce, E. D.; Lavado, R. Comparative cytotoxicity of seven per- and polyfluoroalkyl substances (PFAS) in six human cell lines. *Toxicology* **2022**, *477*, 153281. DOI: https://doi.org/10.1016/j.tox.2022.153281.
(49) Qin, W.; Henneberger, L.; Huchthausen, J.; König, M.; Escher, B. I. Role of bioavailability and protein binding of four anionic perfluoroalkyl substances in cell-based bioassays for quantitative in vitro to in vivo extrapolations. *Environment International* **2023**, *173*, 107857. DOI: https://doi.org/10.1016/j.envint.2023.107857.

(50) Rand, A. A.; Mabury, S. A. Protein binding associated with exposure to fluorotelomer alcohols (FTOHs) and polyfluoroalkyl phosphate esters (PAPs) in rats. *Environmental Science & Technology* **2014**, *48* (4), 2421-2429. DOI: 10.1021/es404390x From NLM.
(51) Rand, A. A.; Rooney, J. P.; Butt, C. M.; Meyer, J. N.; Mabury, S. A. Cellular toxicity associated with exposure to perfluorinated carboxylates (PFCAs) and their metabolic precursors. *Chem Res Toxicol* **2014**, *27* (1), 42-50. DOI: 10.1021/tx400317p From NLM.
(52) Huang, M. C.; Robinson, V. G.; Waidyanatha, S.; Dzierlenga, A. L.; DeVito, M. J.; Eifrid, M. A.; Gibbs, S. T.; Blystone, C. R. Toxicokinetics of 8:2 fluorotelomer alcohol (8:2-FTOH) in male and female Hsd:Sprague Dawley SD rats after intravenous and gavage administration. *Toxicology Reports* **2019**, *6*, 924-932. DOI: https://doi.org/10.1016/j.toxrep.2019.08.009.
(53) PFAS Master List of PFAS Substances. United States Enviormental Protection Agency. https://comptox.epa.gov/dashboard/chemical-lists/pfasmaster (accessed 3/28/2023).
(54) Cocco, C.; Manai, A. L.; Manca, E.; Noli, B. Brain-biomarker changes in body fluids of patients with Parkinsons disease. *International Journal of Molecular Sciences* **2023**, *24* (13). DOI: 10.3390/ijms241310932.
(55) Martí-Martínez, S.; Valor, L. M. A glimpse of molecular biomarkers in huntingtons disease. *International Journal of Molecular Sciences* **2022**, *23* (10). DOI: 10.3390/ijms23105411.
(56) Janigro, D.; Bailey, D. M.; Lehmann, S.; Badaut, J.; O'Flynn, R.; Hirtz, C.; Marchi, N. Peripheral blood and salivary biomarkers of blood–brain barrier permeability and neuronal damage: Clinical and applied concepts. *Frontiers in Neurology* **2021**, *11*, Systematic Review. DOI: 10.3389/fneur.2020.577312.
(57) Bellot, G.; Garcia-Medina, R.; Gounon, P.; Chiche, J.; Roux, D.; Pouysségur, J.; Mazure, N. M. Hypoxia-induced autophagy is mediated through hypoxia-inducible factor induction of BNIP3 and BNIP3L via their BH3 domains. *Molecular and Cellular Biology* **2009**, *29* (10), 2570-2581. DOI: 10.1128/mcb.00166-09 From NLM.
(58) Feng, T.; Lacrampe, A.; Hu, F. Physiological and pathological functions of TMEM106B: a gene associated with brain aging and multiple brain disorders. *Acta Neuropathologica* **2021**, *141* (3), 327-339. DOI: 10.1007/s00401-020-02246-3 From NLM.
(59) Khan, S. F.; Damerell, V.; Omar, R.; Du Toit, M.; Khan, M.; Maranyane, H. M.; Mlaza, M.; Bleloch, J.; Bellis, C.; Sahm, B. D. B.; et al. The roles and regulation of TBX3 in development and disease. *Gene* **2020**, *726*, 144223. DOI: https://doi.org/10.1016/j.gene.2019.144223.
(60) Hellman, M.; Arumäe, U.; Yu, L.-y.; Lindholm, P.; Peränen, J.; Saarma, M.; Permi, P. Mesencephalic astrocyte-derived neurotrophic factor (manf) has a unique mechanism to rescue apoptotic neurons. *Journal of Biological Chemistry* **2011**, *286* (4), 2675-2680. DOI: 10.1074/jbc.M110.146738 (acccessed 2023/05/22).
(61) Su, C.-J.; Feng, Y.; Liu, T.-T.; Liu, X.; Bao, J.-J.; Shi, A.-M.; Hu, D.-M.; Liu, T.; Yu, Y.-L. Thioredoxin-interacting protein induced α-synuclein accumulation via inhibition of autophagic flux: Implications for Parkinson's disease. *CNS Neuroscience & Therapeutics* **2017**, *23* (9), 717-723, https://doi.org/10.1111/cns.12721. DOI: https://doi.org/10.1111/cns.12721 (acccessed 2023/05/22).
(62) Adamson, E. D.; Mercola, D. Egr1 Transcription Factor: Multiple Roles in Prostate Tumor Cell Growth and Survival. *Tumor Biology* **2002**, *23* (2), 93-102. DOI: 10.1159/000059711 (acccessed 5/23/2023).
(63) Mouw, J. K.; Ou, G.; Weaver, V. M. Extracellular matrix assembly: a multiscale deconstruction. *Nature Reviews Molecular Cell Biology* **2014**, *15* (12), 771-785. DOI: 10.1038/nrm3902 From NLM.

(64) Diana, P.; Carvalheira, G. M. G. Niban1, exploring its roles in cell survival under stress context. *Frontiers in Cell and Developmental Biology* **2022**, *10*, Review. DOI: 10.3389/fcell.2022.867003.
(65) Preston, G. A.; Lyon, T. T.; Yin, Y.; Lang, J. E.; Solomon, G.; Annab, L.; Srinivasan, D. G.; Alcorta, D. A.; Barrett, J. C. Induction of apoptosis by c-Fos protein. *Molecular and Cellular Biology* **1996**, *16* (1), 211-218. DOI: 10.1128/mcb.16.1.211 From NLM.
(66) Liao, C.; Wang, T.; Cui, L.; Zhou, Q.; Duan, S.; Jiang, G. Changes in synaptic transmission, calcium current, and neurite growth by perfluorinated compounds are dependent on the chain length and functional group. *Environmental Science & Technology* **2009**, *43* (6), 2099-2104. DOI: 10.1021/es802985e.
(67) Zhao, H.; Xie, J.; Wu, S.; Sánchez, O. F.; Zhang, X.; Freeman, J. L.; Yuan, C. Pre-differentiation exposure of PFOA induced persistent changes in DNA methylation and mitochondrial morphology in human dopaminergic-like neurons. *Environmental Pollution* **2022**, *308*, 119684. DOI: https://doi.org/10.1016/j.envpol.2022.119684.
(68) Zoodsma, J. D.; Boonkanon, C.; Running, L.; Basharat, R.; Atilla-Gokcumen, G. E.; Aga, D. S.; Sirotkin, H. I. Perfluorooctane Sulfonate (PFOS) Negatively Impacts Prey Capture Capabilities in Larval Zebrafish. *Environ Toxicol Chem* **2023**. DOI: 10.1002/etc.5819 From NLM Publisher.
(69) Rehn, M.; Olsson, A.; Reckzeh, K.; Diffner, E.; Carmeliet, P.; Landberg, G.; Cammenga, J. Hypoxic induction of vascular endothelial growth factor regulates murine hematopoietic stem cell function in the low-oxygenic niche. *Blood* **2011**, *118* (6), 1534-1543. DOI: 10.1182/blood-2011-01-332890 From NLM.
(70) Liu, D.; Hu, Z.; Jiang, J.; Zhang, J.; Hu, C.; Huang, J.; Wei, Q. Five hypoxia and immunity related genes as potential biomarkers for the prognosis of osteosarcoma. *Scientific Reports* **2022**, *12* (1), 1617. DOI: 10.1038/s41598-022-05103-3.
(71) Janus, P.; Toma-Jonik, A.; Vydra, N.; Mrowiec, K.; Korfanty, J.; Chadalski, M.; Widłak, P.; Dudek, K.; Paszek, A.; Rusin, M.; et al. Pro-death signaling of cytoprotective heat shock factor 1: upregulation of NOXA leading to apoptosis in heat-sensitive cells. *Cell Death & Differentiation* **2020**, *27* (7), 2280-2292. DOI: 10.1038/s41418-020-0501-8.
(72) Ikeda, S.; Abe, F.; Matsuda, Y.; Kitadate, A.; Takahashi, N.; Tagawa, H. Hypoxia-inducible hexokinase-2 enhances anti-apoptotic function via activating autophagy in multiple myeloma. *Cancer Science* **2020**, *111* (11), 4088-4101. DOI: 10.1111/cas.14614 From NLM.
(73) Lauer, V.; Grampp, S.; Platt, J.; Lafleur, V.; Lombardi, O.; Choudhry, H.; Kranz, F.; Hartmann, A.; Wullich, B.; Yamamoto, A.; et al. Hypoxia drives glucose transporter 3 expression through hypoxia-inducible transcription factor (HIF)–mediated induction of the long noncoding RNA NICI. *Journal of Biological Chemistry* **2020**, *295* (13), 4065-4078. DOI: https://doi.org/10.1074/jbc.RA119.009827.
(74) Tirado-Hurtado, I.; Fajardo, W.; Pinto, J. A. DNA damage inducible transcript 4 gene: The switch of the metabolism as potential target in cancer. *Frontiers in Oncology* **2018**, *8*, Review. DOI: 10.3389/fonc.2018.00106.
(75) Vestergaard, M. B.; Jensen, M. L.; Arngrim, N.; Lindberg, U.; Larsson, H. B. Higher physiological vulnerability to hypoxic exposure with advancing age in the human brain. *Journal of Cerebral Blood Flow & Metabolism* **2020**, *40* (2), 341-353. DOI: 10.1177/0271678x18818291 From NLM.

(76) Santos, M.; Fidalgo, A.; Varanda, A. S.; Oliveira, C.; Santos, M. A. S. tRNA Deregulation and Its Consequences in Cancer. *Trends in Molecular Medicine* **2019**, *25* (10), 853-865. DOI: https://doi.org/10.1016/j.molmed.2019.05.011.
(77) Wei, Z.; Liu, X.; Cheng, C.; Yu, W.; Yi, P. Metabolism of amino acids in cancer. *Frontiers in Cell and Developmental Biology* **2020**, *8*, 603837. DOI: 10.3389/fcell.2020.603837 From NLM.
(78) Fréminet, A. Carbohydrate and amino acid metabolism during acute hypoxia in rats: blood and heart metabolites. *Comparative Biochemistry and Physiology Part B: Comparative Biochemistry* **1981**, *70* (3), 427-433. DOI: https://doi.org/10.1016/0305-0491(81)90277-7.